Noise-induced vortex reversal of self-propelled particles

Hanshuang Chen[1,2] and Zhonghuai Hou[1,*]

[1]*Hefei National Laboratory for Physical Sciences at Microscales & Department of Chemical Physics, University of Science and Technology of China, Hefei 230026, People's Republic of China*

[2]*School of Physics and Material Science, Anhui University, Hefei 230039, People's Republic of China*

(Received 16 April 2012; revised manuscript received 25 August 2012; published 12 October 2012)

We report an interesting phenomenon of noise-induced vortex reversal in a two-dimensional system of self-propelled particles (SPPs) with soft-core interactions. With the aid of forward flux sampling, we analyze the configurations along the reversal pathway and thus identify the mechanism of vortex reversal. We find that the reversal exhibits a hierarchical process: those particles at the periphery first change their motion directions, and then more inner layers of particles reverse later on. Furthermore, we calculate the dependence of the average reversal rate on noise intensity D and the number N of SPPs. We find that the rate decreases exponentially with the reciprocal of D. Interestingly, the rate varies nonmonotonically with N and a local minimal rate exists for an intermediate value of N.

DOI: 10.1103/PhysRevE.86.041122 PACS number(s): 05.40.−a, 05.65.+b, 87.18.Tt, 64.60.−i

I. INTRODUCTION

In recent years, the collective dynamics of self-propelled particles (SPPs) has been a subject of intense research due to the potential implications in biology, physics, and engineering (see [1,2] for recent reviews). Examples of SPPs are abundant including traffic flow [3], birds flocks [4,5], insects swarms [6,7], bacteria colonies [8,9], and active granular media [10,11], just to list a few. Especially, inspired by the seminal work of Vicsek *et al*. [12], many theoretical and experimental studies reported that various systems of SPPs can exhibit a wealth of emergent nonequilibrium patterns like swarming, clustering, and vortex [13–19].

A fascinating phenomenon about SPPs is that they can abruptly change their collective motion pattern, which may be induced by either intrinsic stochasticity such as error in communication among SPPs or a response to an external influence such as a predator. For example, a recent experiment showed that marching locusts can suddenly switch their direction without any change in the external environment [6]. Later, the experimental results were further explained theoretically by mathematical modeling, highlighting the nontrivial role of randomness or noise on this transition [20]. Also, noise-induced transitions between translational motion and rotational motion of SPPs have been observed [21–24]. However, there are still many open questions on this research topic that certainly deserves more investigations. In particular, investigation of the mechanisms about these transitions is lacking at present. As we know, identifying the underlying mechanisms is key to understanding and controlling the collective motion of SPPs.

In this paper, we report an interesting phenomenon of noise-induced vortex reversal between two different rotational directions in a two-dimensional model of SPPs interacting via Morse potential [18]. The vortex pattern has been commonly observed in nature, such as fish, ants [25,26], *Bacillus subtilis* [27], *Dictyostelium* cells [28], vibrated polar disks [29], and collectively moving microtubules [30], as well as some related mathematical models [14,17,31,32], including the model used in the present paper [18]. By virtue of a recently developed simulation method of rare events, forward flux sampling (FFS) [33], we analyze the intermediate configurations along the reversal path and compute the average reversal rate. We find an important statistical property of the vortex reversal, that is, the reversal first starts from peripheral particles and then gradually to inner particles, so that almost all particles change their rotational directions. Furthermore, we show that the reversal rate decreases exponentially with the inverse of noise intensity. Interestingly, the rate varies nonmonotonically with the number of particles and a local minimal rate exists.

II. MODEL DESCRIPTION

We consider N identical SPPs in a two-dimensional space with positions $\vec{x}_i$, velocities $\vec{v}_i$ $(i = 1, \ldots, N)$, and unit mass. The equations of motion read [18]

$$\dot{\vec{x}}_i = \vec{v}_i, \tag{1}$$

$$\dot{\vec{v}}_i = (\alpha - \beta|\vec{v}_i|^2)\vec{v}_i - \sum_{j\neq i} \nabla_i U(|\vec{x}_i - \vec{x}_j|) + \sqrt{2D}\vec{\xi}_i, \tag{2}$$

where the first and second terms on the right hand side (rhs) of Eq. (2) represent self-propelled force and friction force, respectively, and the third term is pair interaction among SPPs given by the generalized Morse potential

$$U(|\vec{x}_i - \vec{x}_j|) = C_r e^{-|\vec{x}_i - \vec{x}_j|/l_r} - C_a e^{-|\vec{x}_i - \vec{x}_j|/l_a}. \tag{3}$$

Here, l_a and l_r represent the attractive and repulsive potential ranges, respectively, C_a and C_r represent their respective amplitudes. The last term on rhs of Eq. (2) is a stochastic force of intensity D that are independent of particle index and satisfy $\langle \xi_{i,m}(t)\rangle = 0$ and $\langle \xi_{i,m}(t)\xi_{j,n}(t')\rangle = \delta_{ij}\delta_{mn}\delta(t - t')$ with $i, j \in 1, \ldots, N$; $m, n \in x, y$. Note that for $D = 0$ our model recovers to the original one proposed by D'Orsogna *et al*. in [18].

The model exhibits diverse dynamic patterns for different model parameters, such as clumps, rings, and vortex. Here we set $\alpha = 1.0$, $\beta = 0.5$, $l_a = 2.0$, $l_r = 0.5$, $C_a = 0.6$, and

*hzhlj@ustc.edu.cn

 ©2012 American Physical Society

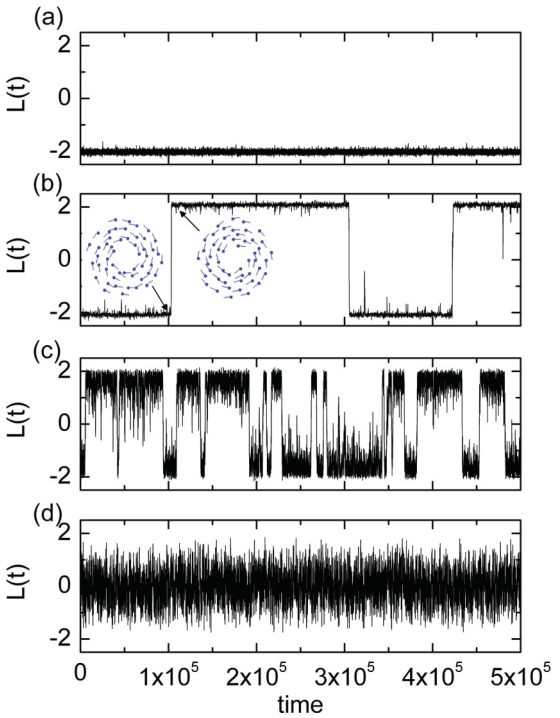

FIG. 1. (Color online) Long-time evolutions of $L(t)$ at four different noise intensity: $D = 0.32$ (a), $D = 0.37$ (b), $D = 0.40$ (c), and $D = 0.46$ (d). Time series in (b) and (c) show several noise-induced vortex reversals. The inset in (b) depicts two typical stable configurations of SPPs: vortex with CW rotation ($L < 0$) and CCW rotation ($L > 0$). The number of particles is $N = 40$.

$C_r = 1.0$. This set corresponds to the case of the vortex. However, due to the catastrophic characteristic of the pair potential between particles, in the $N \to \infty$ limit particles will collapse and thus the vortex pattern will become unstable [18]. Therefore, the following observation on vortex reversal will be just a finite-size effect. To distinguish two different rotational directions of vortex, we define an average angular momentum of particles $\vec{L}(t)$ as $\vec{L}(t) = \frac{1}{N}\sum_{i=1}^{N} \vec{L}_i(t)$, where $\vec{L}_i(t) = \vec{x}_i(t) \times \vec{v}_i(t)$ is the angular momentum of particle i at time t. Since particles' motions are confined to a two-dimensional space in our model, the direction of the vector $\vec{L}$ can only be perpendicular to the motion plane, i.e., $\vec{L} = L\vec{e}_z$ with the unit vector $\vec{e}_z$ orthogonal to the plane of motion. Thus, the sign of L can distinguish the rotational directions of vortex: $L < 0$ and $L > 0$ indicate clockwise (CW) and counterclockwise (CCW) vortex, respectively.

III. SIMULATION DETAILS

Equations (1) and (2) are numerically integrated using a fourth order Adams-Bashforth method [34] with a time step $dt = 0.01$ and allowing particles an infinite range of motion. In order to observe the noise-induced effect on vortex motion, we show in Fig. 1 long-time evolutions of $L(t)$ by brute-force simulations at $N = 40$ at four different noise intensity: $D = 0.32$ (a), $D = 0.37$ (b), $D = 0.40$ (c), and $D = 0.46$ (d). For $D = 0.32$, the system is in vortex pattern and its rotational direction does not change within our observation time. In this

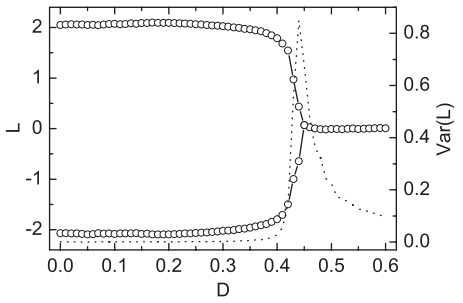

FIG. 2. Average angular momentum L of SPPs (hollow circles) and its variance $\langle L(t)^2\rangle - \langle L(t)\rangle^2$ (dotted line) as a function of noise intensity D. The number of particles is $N = 50$.

case, a longer observation time is desirable to observe the nontrivial effect of this weak noise. For a larger D, $D = 0.37$, one can observe that noise can induce the sudden transitions of SPPs between two different rotational directions. The inset in Fig. 1(b) depicts two typical configurations of SPPs: vortex with CW and CCW rotations. If D is increased to $D = 0.40$, the noise-induced transitions become more frequent. Further increasing D to $D = 0.46$, the value of L fluctuates around zero, implying that the vortex pattern is destroyed by the strong noise and the motion of SPPs become disordered.

In Fig. 2, we plot the steady values of L as a function of D. To obtain the steady values, we start from 20 different initial configurations chosen randomly, and run 2×10^6 time steps, where the first 10^6 time steps are discarded and the following 10^6 time steps are used to calculate the steady value of L. In the presence of a weak noise, the absolute value of L is always much larger than zero, implying that the vortex pattern is stable and the system certainly falls into either of two branches depending on initial configurations. By increasing D, the vortex will be destroyed and the motion of SPPs become disordered ($L = 0$) if D is larger than a critical value $D_c \simeq 0.44$. We also note that the fluctuation of $L(t)$, $\langle L(t)^2\rangle - \langle L(t)\rangle^2$ is maximal at $D = D_c$ (see the dotted line in Fig. 2), where $\langle\cdot\rangle$ denotes the average over time. Moreover, we have changed the number of particles from 40 to 180, and found that the results are similar and the value of D_c is almost unchanged. Therefore, in this paper D is set be less than D_c to study noise-induced vortex reversal.

From Fig. 1, one can see that noise-induced reversal events occur rarely and the average waiting time between reversal events is very long, especially for the case of weak noise. In this situation, conventional brute-force simulation becomes highly inefficient. To overcome this difficulty, we will use the FFS method of Allen and co-workers [33] to compute the rate of vortex reversal and evaluate statistical properties of the reversal path, which is the main purpose of the present work.

The FFS method was designed to study rare events both in and out of equilibrium. This method first defines an order parameter to distinguish between the initial state A and the final state B, and then uses a series of interfaces to force the system from A to B in a ratchetlike manner. In this paper, it is convenient to select L as the order parameter, and consider the CW vortex as A and the CCW vortex as B without loss of generality since these two states are equivalent in our model.

We consider that the system is in state A if $L < L_0$ and it is in state B if $L > L_m$. A series of nonintersecting interfaces L_i $(0 < i < m)$ lie between states A and B, such that any path from A to B must cross each interface without reaching L_{i+1} before L_i. Starting from the configuration of the CW vortex, we first run a long-time simulation to give an estimate of the flux $\bar{\Phi}_{A,0}$ escaping from the basin of A and generate a collection of configurations corresponding to crossings of interface L_0. The next step is to choose a configuration from this collection at random and use it to initiate a trial run which is continued until it either reaches L_1 or returns to L_0. If L_1 is reached, store the configuration of the end point of the trial run. Repeat this step, each time choosing a random starting configuration from the collection at L_0. The fraction of successful trial runs gives an estimate of the probability of reaching L_1 without going back into A, $P(L_1|L_0)$. This process is repeated, step by step, until L_M is reached, giving the probabilities $P(L_{i+1}|L_i)$ $(i = 1, \ldots, m-1)$. Finally, we get the transition rate R of vortex reversal,

$$R = \bar{\Phi}_{A,0} P(L_m|L_0) = \bar{\Phi}_{A,0} \prod_{i=0}^{m-1} P(L_{i+1}|L_i), \quad (4)$$

where $P(L_M|L_0)$ is the probability of reaching L_m from L_0 without going into A. For detailed descriptions of the FFS method see Ref. [35].

By storing SPP configurations $\{\vec{x}_i, \vec{v}_i\}$ $(i = 1, \ldots, N)$ at each interface of FFS sampling, one can identify the statistical properties of the vortex reversal pathway. All results below are obtained by averaging ten independent FFS samplings. In each FFS sampling, 1000 configurations are stored at each interface to analyze the statistical properties of the configurations. Due to slow random drift of vortex as a whole, the positions of center of mass for these 1000 configurations are slightly different. In order to facilitate the analysis of radial features of the configurations, all quantities are calculated in the center-of-mass coordinate.

IV. RESULTS

In Fig. 3, we show the velocity field of SPP at six different interfaces along the pathway of vortex reversal. The velocity field is indicated by the arrows in Fig. 3, which is obtained by averaging 1000 configurations of particles stored at each FFS interface. Figures 3(a) and 3(f) show the velocity field before and after the reversal, indicating that the system is in stable vortex with CW and CCW rotation, respectively, while Figs. 3(b)–3(e) show the intermediate processes of the reversal. One can clearly observe that along the pathway of vortex reversal the velocity field gradually changes its sign from the periphery to the center of the vortex. That is to say, vortex reversal first starts from peripheral particles and then gradually to inner particles, and finally almost all particles change original rotational directions.

Further information on the pathway of vortex reversal is provided by the radial distributions of average angular momentum $L(r)$ and average angular velocity $\omega(r)$, where r is the distance to the center of mass. In Fig. 4, we plot $L(r)$ and $\omega(r)$ for five different interfaces along the pathway of vortex reversal. From the variations of $L(r)$ and $\omega(r)$ with interfaces one can observe the whole process of the vortex reversal.

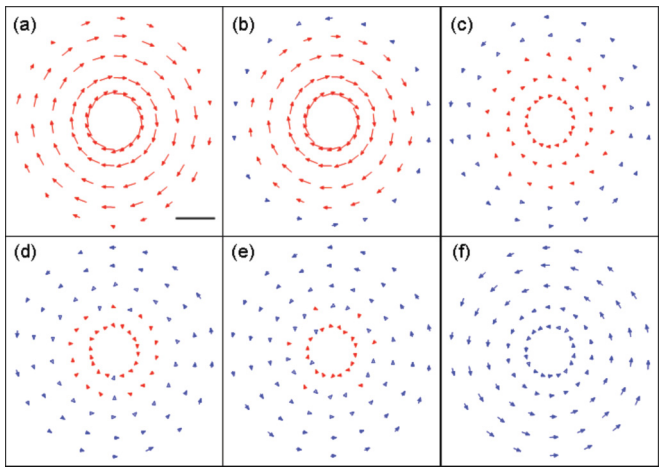

FIG. 3. (Color online) The velocity field of SPPs at six different FFS interfaces, corresponding to (a) $L = -1.95$, (b) $L = -1.6$, (c) $L = 0$, (d) $L = 0.25$, (e) $L = 0.4$, and (f) $L = 1.0$, respectively. The bar in (a) indicates unit length. Other parameters are $N = 50$ and $D = 0.30$.

Before the reversal ($L = -1.95$) the values of $L(r)$ and $\omega(r)$ are always negative, irrespective of r. That is, the system is in a stable vortex with CW rotation before the reversal. When the reversal happens, for example, for $L = 0$, the values of $L(r)$ and $\omega(r)$ become positive for $r > 1.8$, while for $r < 1.8$ they are always negative. With increasing L this situation further goes until any values of $L(r)$ and $\omega(r)$ become positive. Finally, the vortex rotates with CCW direction. Therefore, this further validates that the property of vortex reversal is that the reversal process starts from the periphery of the vortex. Also, we calculate the radial distributions of density of particles and

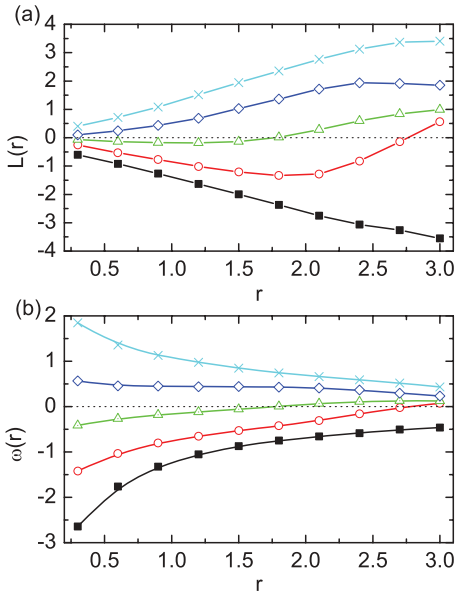

FIG. 4. (Color online) (a) Radial distributions of average angular momentum $L(r)$ and (b) average angular velocity $\omega(r)$ at five different interfaces along the pathway of vortex reversal: $L = -1.95$ (squares), $L = -1.0$ (circles), $L = 0.0$ (triangles), $L = 1.0$ (diamonds), and $L = 1.95$ (crosses). Other parameters are the same as those in Fig. 3.

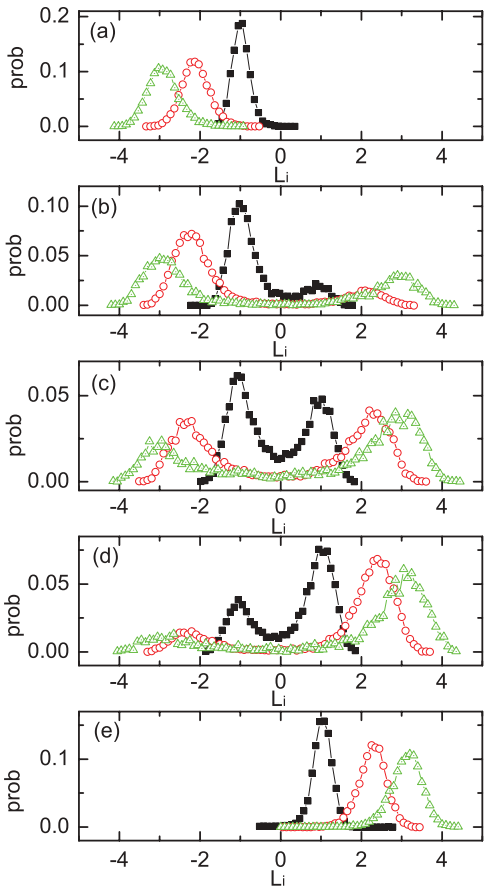

FIG. 5. (Color online) The distributions of angular momentum L_i for those particles with $r \in [0.6,1.0]$ (squares), $r \in [1.6,2.0]$ (circles), and $r \in [2.6,3.0]$ (triangles) at five different FFS interfaces: $L = -1.95$ (a), $L = -1.0$ (b), $L = 0.1$ (c), $L = 1.0$ (d), and $L = 1.95$ (e). Other parameters are the same as those in Fig. 3.

the absolute value of velocity of particles, and find that they do not have a significant difference with the interfaces L.

It is informative to analyze the statistical properties of angular momentum of particles at different distances to the center of mass. In Fig. 5, we show the distributions of L_i of particles at $r \in [0.6,1.0]$ (squares), $[1.6,2.0]$ (circles), and $[2.6,3.0]$ (triangles) at five different FFS interfaces: $L = -1.95$ (a), $L = -1.0$ (b), $L = 0.1$ (c), $L = 1.0$ (d), and $L = 1.95$ (e). An interesting observation is that along the reversal pathway the distributions of L_i change from unimodal to bimodal shape. Before the reversal, the distribution of L_i for particles at each layer is unimodal. During the reversal, the distributions spread to the right and become bimodal. With the progress of the reversal, the relative heights of the two peaks for the distributions vary until the vortex is totally reversed and the distributions become unimodal again. Importantly, as shown in Fig. 5, the loci of the two peaks are coincident with those before and after the reversal. This indicates that all the particles still maintain the rotational property during the process of the reversal, and just adjust their rotational directions. The same results can be also obtained by measuring the distribution of the angular velocity.

Since the vortex reversal is closely related to a barrier-crossing process, it is possible to identify the so-called critical configurations at the top of the barrier. Similar to the definition of critical nucleus for studying nucleation in a first-order phase transition [36], the critical configurations are determined when the so-called committor probability $P_B(i)$ is 0.5, where $P_B(i) = \prod_{j=i}^{m-1} P(L_{j+1}|L_j)$ is easily computed by the FFS sampling. The meaning of $P_B(i)$ is the probability of reaching the B state before returning to the A state starting from the ith FFS interface. Namely, if the system evolves from the critical configurations, there is an equal probability of returning to the CW or CCW vortex. If the rotational directions of the initial and final states are, respectively, CW and CCW, we find that $L \simeq 0.08$ at the critical configurations, that is, the average angular momentum of all particles is slightly larger than zero at the critical configurations. By varying noise intensity D and the number of particles N, the value is almost unchanged. On the contrary, if we swap the rotational directions of the initial and final states, $L \simeq -0.08$ at the critical configurations holds simply due to the rotation symmetry. The results in Fig. 5(c) are very close to the critical configurations. Furthermore, we should note that although the parameters used in Figs. 3–5 are fixed at $N = 50$ and $D = 0.30$, detailed analysis for different N and D has been also performed and the results about the reversal pathway are qualitatively the same.

Another key question in vortex reversal concerns the dependence of average rate R of the reversal on noise intensity D and the number of particles N. In Fig. 6(a) we plot the natural logarithm of the rate $\ln R$ as a function of the inverse of D for different N varying from $N = 40$ to $N = 180$. The value of D we use changes from $D = 0.20$ to $D = 0.40$. The obtained value of R varies from 10^{-5} to 10^{-37} that spans as much as 32 orders of magnitude. If we further increase N or decrease D, simulation will be very time consuming so that our computational power is out of reach. The maximal value of D is set be less than but close to D_c. This is because, as mentioned above, if $D > D_c \simeq 0.44$ vortex pattern will be no longer stable and thus vertex reversal makes no sense. The result in Fig. 6(a) shows that $\ln R$ decreases linearly with $1/D$. Interestingly, the slope for each N differs and it is varied nonmonotonically with N. Furthermore, this result indicates that if our model contains no noise, i.e., the model recovers to the original one in Ref. [18], it does not exhibit vortex reversal, highlighting the nontrivial effect of noise. In Fig. 6(b) we show $\ln R$ as a function of N for different D. Interestingly, we find that R varies nonmonotonically with N. With the increment of N, R first decreases and then increases, and then decreases again. Thus, R has a local minima at $N = 48$ for low D and at $N = 50$ for high D. We should note that, as mentioned above, the vortex pattern is stable only if N is finite. Therefore, the present results do not simply generalize to the infinite-size limit. From Fig. 6(a), one may speculate that there seems to be an effective nonequilibrium potential for describing the collective transition in rotational directions. The potential barrier between the CW vortex and the CCW vortex is fixed if N is unchanged, such that the transition rate follows classical Kramers' law. On the other hand, the nonmonotonic variation trend between R and N implies that a dependence of the effective nonequilibrium potential on N is nontrivial if it exists. However, understanding these results from the view of theoretical analysis, if not infeasible, is at least a complex task at present.

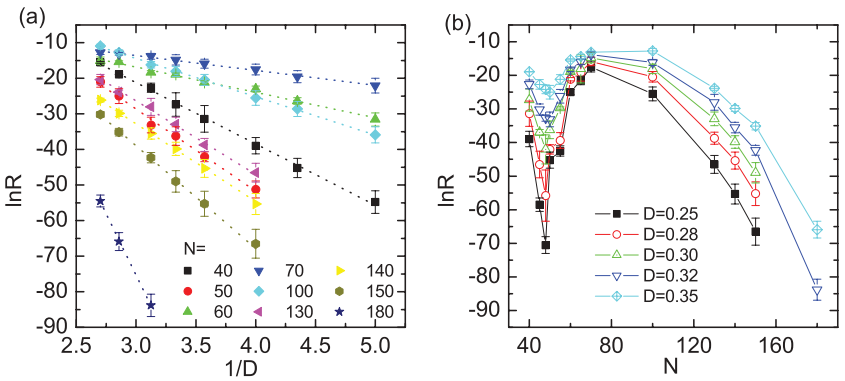

FIG. 6. (Color online) The natural logarithm of rate of vortex reversal ln R as a function of the inverse of noise intensity $1/D$ for different SPP number N (a) and as a function of N for different D (b). The dashed lines in (a) are plotted by linear fitting.

V. DISCUSSION AND CONCLUSIONS

The phenomenon of vortex reversal has been observed in a recent experiment on a monolayer of vibrated polar disks [29]. The experiment showed that these particles can exhibit alternating transitions between the CW and CCW vortex, and the intermediate states between these transitions are not disordered but obviously have the domain shape as the trace of vortex configuration. This may share a similarity with our finding. As shown in the above analysis for the intermediate states, particles during the reversals are also not disordered but still preserve the rotational property. Also, we expect that further experiments can be performed for the scrutiny of the intermediate configurations of particles during reversals. Furthermore, it would be interesting to compare our results with previous findings on one-dimensional models, both experimentally and theoretically, where a swarm of marching particles can suddenly switch the direction of motion due to noise [6,20,37,38]. First, our model is two dimensional such that the analysis for particles at different layers of vortex during the reversals is possible. As shown in this paper, the analysis is essential for the understanding of these reversal events. Besides, our results showed that the transition rate exhibits a complex dependence on the number of particles, significantly different from the case of one-dimensional models where the transition rate decreases exponentially with the number of particles.

In summary, using a two-dimensional model of SPPs interacting via a soft-core potential, we have investigated the mechanism of noise-induced changes of a vortex pattern in the rotational direction. By virtue of the FFS method we analyze the statistical property and compute the rate of the reversal. We find that the reversal process is hierarchical: the process is initially inspired by the peripheral particles, and those particles gradually drive more inner layers of particles into reverse motion directions. On the other hand, we show that the rate of the reversal decreases exponentially with the inverse of noise intensity. Interestingly, the reversal rate depends nonmonotonically on the number of SPPs and a local minimal rate exists at a moderate number of particles. Our findings may provide some new understanding on the transitions of collective patterns of SPPs.

ACKNOWLEDGMENTS

This work was supported by the National Science Foundation of China (Grants No. 11205002, No. 91027012, No. 20933006). Z.H.H. acknowledges support by China National Funds for Distinguished Young Scientists (Grant No. 21125313). H.S.C. acknowledges support by the Doctoral Research Foundation of Anhui University (Grant No. 02303319).

[1] S. Ramaswamy, Annu. Rev. Condens. Matter Phys. **1**, 323 (2010).
[2] T. Vicsek and A. Zafiris, Phys. Rep. **517**, 71 (2012).
[3] D. Helbing, Rev. Mod. Phys. **73**, 1067 (2001).
[4] A. Cavagna, A. Cimarelli, I. Giardina, G. Parisi, R. Santagati, F. Stefanini, and M. Viale, Proc. Natl. Acad. Sci. USA **107**, 11865 (2010).
[5] K. Bhattacharya and T. Vicsek, New J. Phys. **12**, 093019 (2010).
[6] J. Buhl, D. J. T. Sumpter, I. D. Couzin, J. J. Hale, E. Despland, E. R. Miller, and S. J. Simpson, Science **312**, 1402 (2006).
[7] P. Romanczuk, I. D. Couzin, and L. Schimansky-Geier, Phys. Rev. Lett. **102**, 010602 (2009).
[8] L. Angelani, R. Di Leonardo, and G. Ruocco, Phys. Rev. Lett. **102**, 048104 (2009).
[9] H. P. Zhang, A. Be'er, E. L. Florin, and H. L. Swinney, Proc. Natl. Acad. Sci. USA **107**, 13626 (2010).
[10] V. Narayan, S. Ramaswamy, and N. Menon, Science **317**, 105 (2007).
[11] J. Deseigne, O. Dauchot, and H. Chaté, Phys. Rev. Lett. **105**, 098001 (2010).
[12] T. Vicsek, A. Czirók, E. Ben-Jacob, I. Cohen, and O. Shochet, Phys. Rev. Lett. **75**, 1226 (1995).
[13] J. Toner and Y. Tu, Phys. Rev. Lett. **75**, 4326 (1995).
[14] G. Grégoire and H. Chaté, Phys. Rev. Lett. **92**, 025702 (2004).
[15] M. Aldana, V. Dossetti, C. Huepe, V. M. Kenkre, and H. Larralde, Phys. Rev. Lett. **98**, 095702 (2007).
[16] H. Chaté, F. Ginelli, and R. Montagne, Phys. Rev. Lett. **96**, 180602 (2006).
[17] H. Levine, W.-J. Rappel, and I. Cohen, Phys. Rev. E **63**, 017101 (2000).
[18] M. R. D'Orsogna, Y. L. Chuang, A. L. Bertozzi, and L. S. Chayes, Phys. Rev. Lett. **96**, 104302 (2006).

[19] F. Peruani, T. Klauss, A. Deutsch, and A. Voss-Boehme, Phys. Rev. Lett. **106**, 128101 (2011).
[20] C. A. Yates, R. Erban, C. Escudero, I. D. Couzin, J. Buhl, I. G. Kevrekidis, P. K. Maini, and D. J. T. Sumpter, Proc. Natl. Acad. Sci. USA **106**, 5464 (2009).
[21] A. S. Mikhailov and D. H. Zanette, Phys. Rev. E **60**, 4571 (1999).
[22] U. Erdmann, W. Ebeling, and A. S. Mikhailov, Phys. Rev. E **71**, 051904 (2005).
[23] A. Kolpas, J. Moehlis, and I. G. Kevrekidis, Proc. Natl. Acad. Sci. USA **104**, 5931 (2007).
[24] J. Strefler, U. Erdmann, and L. Schimansky-Geier, Phys. Rev. E **78**, 031927 (2008).
[25] J. K. Parrish, S. V. Viscido, and D. Grunbaum, Biol. Bull. **202**, 296 (2002).
[26] D. J. T. Sumpter, Philos. Trans. R. Soc. B **361**, 5 (2006).
[27] A. Czirók, E. Ben-Jacob, I. Cohen, and T. Vicsek, Phys. Rev. E **54**, 1791 (1996).
[28] W.-J. Rappel, A. Nicol, A. Sarkissian, H. Levine, and W. F. Loomis, Phys. Rev. Lett. **83**, 1247 (1999).
[29] J. Deseigne, S. Léonard, O. Dauchot, and H. Chaté, Soft Matter **8**, 5629 (2012).
[30] Y. Sumino1, K. H. Nagai, Y. Shitaka, D. Tanaka, K. Yoshikawa, H. Chaté, and K. Oiwa, Nature (London) **483**, 448 (2012).
[31] Y. L. Duparcmeur, H. Herrmann, and J. P. Troadec, J. Phys. I **5**, 1119 (1995).
[32] J. Hemmingsson, J. Phys. A: Math. Gen. **28**, 4245 (1995).
[33] R. J. Allen, P. B. Warren, and P. R. ten Wolde, Phys. Rev. Lett. **94**, 018104 (2005).
[34] G. H. Golub and J. M. Ortega, *Scientific Computing and Differential Equations: An Introduction to Numerical Methods* (Academic, New York, 1992).
[35] R. J. Allen, C. Valeriani, and P. R. ten Wolde, J. Phys.: Condens. Matter **21**, 463102 (2009).
[36] A. C. Pan and D. Chandler, J. Phys. Chem. B **108**, 19681 (2004).
[37] A. Czirók, A.-L. Barabási, and T. Vicsek, Phys. Rev. Lett. **82**, 209 (1999).
[38] O. J. O. Loan and M. R. Evans, J. Phys. A: Math. Gen. **32**, L99 (1999).